Electrochimica Acta xxx (2015) xxx–xxx

Contents lists available at ScienceDirect

Electrochimica Acta

journal homepage: www.elsevier.com/locate/electacta

Theoretical Evaluation of Electron Transport in Aniline Tetramer-based Dye-sensitized Solar Cells

Shozo Yanagida [a,*], Kazuhiro Manseki [b], Hiroshi Segawa [c]

[a] Osaka University, Suita, Osaka, Japan 565-0871
[b] Gifu University, Yanagido, Gifu, Japan 501-1193
[c] University of Tokyo, RCAST, Hongo, Tokyo, Japan 153-8904

ARTICLE INFO

Article history:
Received 5 October 2014
Received in revised form 5 April 2015
Accepted 6 April 2015
Available online xxx

Key words:
DFT-based molecular modeling
orbital energy
non-covalent molecular orbitals
van der Waals and Coulombic interactions
SOMO
electron hopping

ABSTRACT

The essential electron transporting function of EPAT in phenyl-capped aniline tetramer (EPAT)/*tert*-butylpyridine (TBP)-based dye-sensitized solar cells (DSC) is evaluated by density functional theory (DFT). DFT-based molecular modeling coupled with molecular mechanics optimization reveal that EPAT molecules *in-situ* self-organizes to dimeric molecular complexes through van der Waals and Coulombic interactions. TBP molecules assist to form TBP-hydrogen-bonded EPAT complexes, $(EPAT\text{-}H\text{-}TBP)_2$ and $(EPAT\text{-}H\text{-}2TBP)_2$. The molecular complexes have stacked structures as well, and the electron-accepted states of radical anions, $(EPAT\text{-}H\text{-}TBP)_2^{\cdot -}$ and $(EPAT\text{-}H\text{-}2TBP)_2^{\cdot -}$ give narrow band gaps (0.26∼0.28 eV), and the singly occupied molecular orbitals (SOMO) are comparable in configurations with the lowest unoccupied molecular orbital (LUMO). We understand that electron in photo-irradiated EPAT/TBP phase should transport effectively by hopping on SOMO of $(EPAT\text{-}H\text{-}TBP)_2^{\cdot -}$ and $(EPAT\text{-}H\text{-}2TBP)_2^{\cdot -}$.

1. Introduction

As vividly acknowledged by Nobel Prize in chemistry 2013 [1], remarkable advance of hardware and software in computational molecule orbital chemistry enable experimental chemists to evaluate molecular structures not only of covalent bond molecules but also molecules that are non-covalently bonded by hydrogen bonding and, van der Waals (vdW) and Coulombic (Clb) interactions. Particularly, density functional theory (DFT) simulates almost all molecules that are composed of any elements in periodic table. In addition, molecular orbital calculations are applicable to active molecules such as electron accepted and electron-donated molecules called as radical anions and radical cations. Characterizations of bond lengths, Mulliken charge, dipole, and molecular orbital energy structures are all informative for understanding and evaluation of molecular systems. Accordingly, DFT-based molecular modeling for molecular orbital integrated systems like dye-sensitized solar cells (DSC) becomes instructive and predictive in evaluating photovoltaic performance.

We recently reported that DSC work effectively when iodide-based electrolyte solution is replaced by a fluid solution of phenyl-capped aniline tetramer (EPAT). The fluid solution is composed of EPAT (0.04 M), and *tert*-butylpyridine (TBP, 0.04∼1.0 M), and furthermore, Z-907 (cis-bis(isothiocyanato)(2,20-bipyridyl-4,40-dicarboxylato)(2,20-bi-pyridyl-4,40-di-nonyl ruthenium(II))) is indispensable as an effective sensitizer.

Important findings are summarized as follows, 1) open circuit voltage (Voc) is dramatically improved, 2) Voc and fill factor (ff) are optimized by changing ratios of TBP to EPAT up to 10, and 3) the optimized Jsc is obtainable at 8-μm thickness, in other words, diffusion length is around 8 μm. In the preceding paper, these observations were rationalized by DFT-based molecular modeling of interfaces of Z907 and EPAT molecules. The non-covalent molecular orbital interactions of EPAT with *n*-nonyl and SCN groups in Z907 were proposed to contribute to one-way electron transport at Z907/EPAT interfaces. As for TBP effects on DSC, TBP-hydrogen-bonding with EPAT was assumed to enhance solubility of EPAT in TBP-contain butyronitrile in view of dipole moment increment, enabling EPAT molecules to infiltrate deep inside of mesoporous nc-TiO_2 layers [2].

Theoretical non-covalently-bonded molecular orbital modeling has now revealed that EPAT itself associates each other. The electron transport function of the TPB-assisted EPAT stack-association systems are evaluated by assuming that hopping electron should diffuse through electron-accepted molecular orbitals, i.e., through singly occupied molecular orbital (SOMO) of the electron-accepted-state radical anions.

* Corresponding author. Tel.: +81-90-1073-9244.
E-mail address: yanagida@mls.eng.osaka-u.ac.jp (S. Yanagida).

http://dx.doi.org/10.1016/j.electacta.2015.04.026
0013-4686/

2. Experimental

2.1. Computational Methods for non-covalently bonding molecules

Software of *Spartan'14* (Wavefunction, Inc, CA) is installed on VAIO Model SVP132A1CN, Intel(R) core(TM) i7-4500U CPU and on VAIO PC-Z (Intel core 2 Duo processor T9900, system memory (RAM) 8G and hard disk drive, SSD 128, 2GB). As for orbital configurations, HOMO is shown by solid, LUMO by mesh, LUMO (+1) by dots, SOMO by transparent solid, and spin density by white solid in electron density map. As for color in electrostatic potential map and in electron density map, red is negative, green neutral and blue positive qualitatively.

2.2. Correctness verification of DFT-simulated orbital energy levels as theoretical experiments using packing unit of semiconducting rubrene crystal,

Rubrene crystal is well known to be semiconducting as an excellent organic semiconductor. [3,4] The x-ray single-crystal packing unit structure of rubrene is obtained from the Cambridge Structural Database (CSD) (QQQCIG13). All DFT calculations are performed to obtain total energy of each rubren component after freezing heavy atoms of the components while optimizing C—H bonds in crystalline-state rubrene group. The optimized structures are calculated for the equilibrium geometry using Spartan'14 (DFT, B3LYP functional, the 6-31G* basis set) (Table S1, Table S2, Fig. S1). The Spartan'14 displays energy diagrams of the twelve high occupied and the two low unoccupied molecular orbitals. We denote the highest occupied and the lowest unoccupied molecular orbitals by HOMO and LUMO, respectively. As for electron-accepted models, i.e., radical anions of the rubrene, their orbital energy diagrams are shown in two ways, affixed "a-" and "b-" because the radical anions have two wave functions, corresponding to different spins. By a-HOMO and a-LUMO we indicate singly occupied molecular orbital (SOMO) and LUMO of the radical anion components, since the configurations of a-HOMO are almost the same as not only the SOMO configurations but also the LUMO configurations of the neutral states. The energy gap of the radical anions is verified to become narrow judging from energy difference between SOMO and LUMO. The spin density is verified to distribute on SOMO (Table S2).

The rubrene units, dimers, trimer, tetramer and pentamer in the crystal is not stable enough when judged from ΔE as difference of total energy (E). The stack dimer is optimized by molecular mechanics (MMFF operation) and calculated for the energetically stabilized equilibrium geometry (Fig. 1S and Table S3). The stacked dimer at equilibrium geometry is successfully modeled to have strong tendency to interact each other because of degenerate HOMO and LUMO configurations. The molecular orbital structure of the radical anion model has the comparable SOMO configuration and the narrow energy gap as well as the stacked dimer model in the crystal (Table S3).

2.2.1. EPAT-H-TBP and EPAT-H-2TBP models

TBP and EPAT are manually arranged to have hydrogen bonding at one side or at both side, and optimized by molecular mechanics (MMFF operation in *Spartan'14*). The optimized structures are calculated for the equilibrium geometry using DFT (Fig. S2).

2.2.2. $(EPAT\text{-}H\text{-}TBP)_2$ and $(EPAT\text{-}H\text{-}2TBP)_2$ models

two EPAT-H-TBP are allowed to interact one another via van der Waals and Coulombic interaction. The dimer structure is optimized by molecular mechanics (MMFF), and calculated by DFT for the equilibrium geometry (Fig. S3). As for Two TBP molecules are manually hydrogen bonded to the equilibrium structure of (EPAT-H-TBP) 2 and the structure is modeled by single point energy calculation.

2.2.3. Radical anion models; $[(EPAT\text{-}H\text{-}TBP)_2]^-$ and $(EPAT\text{-}H\text{-}2TBP)_2]^-$

The radical cations are modeled by single point energy calculations of the model structures subject to total charge of minus one and one unpaired electron. Molecular orbital energy structures, SOMO, spin density, energy gap between SOMO and LUMO (a-LUMO) and total energy are analyzed for the defined problem of conductivity.

Nano-TiO_2 model: The file of mol2 of ($Ti_{19}O_{18}H(OH)$) was given by Yamashsita and Jono, and analyzed (Table S3) [5].

3. Results and Discussion

3.1. DFT-based molecular modeling of EPAT stack-association

The equilibrium geometry of EPAT (The symmetrical EPAT is energetically stable than unsymmetrical, and employed for DFT-based molecular modeling) suggests that the frontier orbitals, HOMO and LUMO, delocalize symmetrically, and that the hydrogen atoms at periphery have positive charge and the carbon in phenyl ring and nitrogen atoms negative charge (Fig. S2). On DFT-based molecular modeling of EPAT self-association, the MMFF-optimized EPAT stacked structure converges to the equilibrium state of an EPAT stack dimer (Fig. 1). Thermodynamic energy change (ΔE) suggests that the formation of EPAT stack dimer is exothermic (Table S4). Comparison of van der Waals distances between EPAT

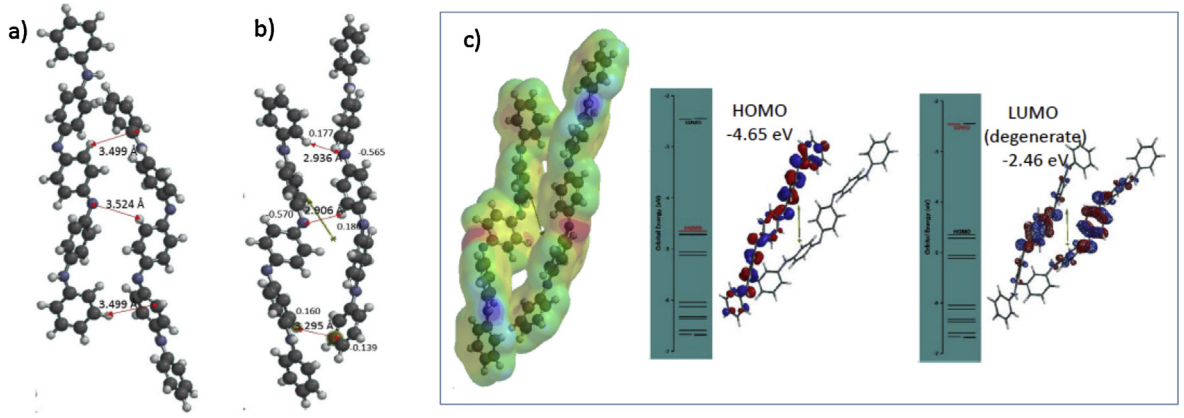

Fig. 1. DFT-based molecular modeling of EPAT self-association to EPAT stack dimer and the 3D structure at the equilibrium geometry. a) The MMFF-optimized EPAT association structure, b) Equilibrium geometry of EPAT stack dimer, c) Electrostatic potential map of the dimer.

Please cite this article in press as: S. Yanagida, et al., Theoretical Evaluation of Electron Transport in Aniline Tetramer-based Dye-sensitized Solar Cells, Electrochim. Acta (2015), http://dx.doi.org/10.1016/j.electacta.2015.04.026